HIGH ORDER FEEDBACK DESIGN TO IMPROVE ROBOT PERFORMANCE

O. Yaniv[1,2], M. Nagurka[3], S. Safonov[2], and T. Flash[4]

[1]*Faculty of Eng., Tel-Aviv University, Tel-Aviv 69978, Israel, yaniv@eng.tau.ac.il*
[2]*Elmo Position Control Ltd., 1 Shidlovskey St., POB 13081, Yavne 81101 Israel*
[3]*Dept. of Mechanical & Industrial Eng., Marquette University, Milwaukee, WI 53201 USA*
[4]*Computer Science & Applied Math., The Weizmann Institute, Rehovot 76100, Israel*

Abstract: In comparison to *PI* and *PID* controllers, a higher order "advanced" controller is shown to improve the performance of an experimental robot for speed and position control applications. The advanced controller attains a higher bandwidth, lower settling time and better disturbance rejection, while the increased performance costs little in sensor noise amplification. *Copyright 2002 IFAC*

Keywords: Identification, robust control, PID control, Flexible arms, MIMO.

1. INTRODUCTION

The design of controllers for robotic applications and for electrical actuators has been studied extensively, and commercial controllers for robots and motors are readily available. In real-world applications, the controller of a servo system must meet multiple objectives. For example, the controller must accelerate the servo system to reach the target speed as fast as possible. After reaching the target speed, it must regulate the system to minimize speed variation. The controller must provide sufficient robustness to ensure that the stability and performance of the system are insensitive to payload variation. Additionally, the synthesized current command must remain smooth enough so it can be achieved by the current amplifier without saturating or, if it saturates, recover quickly. Furthermore, the controller must avoid generating excessive stresses (due to torque) that might cause failure or shorten the system life.

The most common controllers are proportional *P*, proportional-integral *PI*, and proportional-integral-derivative *PID* controllers. They have been adopted widely in industry. The primary advantage of *P*, *PI* and *PID* controllers is their inherent simplicity in that they have few "free" parameters, the gains, that can be tuned effectively using straightforward methods. In addition to "guideline-based" methods (e.g., Zeigler-Nichols method relying on open and closed-loop tests of the plant), optimization-based and other methods have been proposed for tuning (Mann, et al, 2001).

Classical controllers are effective for controlling relatively benign systems, e.g., systems with low or moderate performance requirements, systems with linear or near linear dynamics and with sufficient damping, systems with low uncertainty, and multi-dimensional systems with minimal cross-talk among the axes. However, the performance of these systems and especially of more challenging systems is limited using classical controllers, and can be improved by adopting more complicated controllers.

The most significant drawback of classical controllers is their poor high-frequency attenuation. Classical controllers also have problems in systems with resonant behavior. Researchers and practitioners who have encountered difficulties have developed nonlinear controllers that have attempted to extend the *PID* structure using neural networks, adaptive self-tuning control, fuzzy logic control, and combinations of these approaches. Some practitioners have found it attractive to extend *PID* controllers by adding notch and low-pass filters.

Advanced controllers can push the tracking and disturbance attenuation performance to the physical limits of the system. They can achieve the desired performance even in systems with flexibility and limited damping, and in systems with less than ideal actuators and degraded or low-quality sensors. For the same system dynamics (mechanics-sensors set), advanced controllers can increase the speed range in which accurate motions are possible, increase the bandwidth and handle more uncertainty, and lower the amplitude of existing limit cycles, if present.

1.1 Application System

This paper explores controller designs for a planar two-link robot, shown in Fig. 1. In this robot, similar to a SCARA-configuration robot and designed originally by Hogan (Mussa-Ivaldi, et al, 1985; Faye, 1986) for human-machine interaction studies (Mussa-Ivaldi, et al, 1985; Flash, 1987; Won and Hogan, 1995), each joint is driven by a DC servomotor. The motors have output shafts that are co-axial with the axis of rotation of the inner link. For each motor, a tachometer measures the shaft speed and an encoder measures the motor shaft angle. The inner link (link 1) is attached directly to the output shaft of the upper motor (motor 1), whereas the outer link (link 2) is driven (by motor 2) through a four-bar linkage.

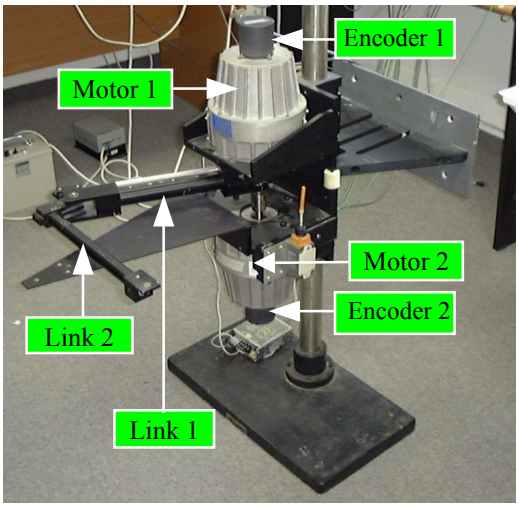

Fig. 1. Experimental two-link robot. (Dimensions are 36.1cm for link 1 and 33.2cm for link 2.)

A general view of the control structure for each motor is shown in Fig. 2. For a motor (the plant) with shaft angle, $\theta(t)$, driven by current, $i(t)$, the goal in speed control is to have the shaft speed, $\dot{\theta}(t)$, follow a given or desired trajectory, $\dot{\theta}_T(t)$. The standard approach is to employ a feedback structure depicted in the inner loop of the block diagram of Fig. 2 (dashed box).

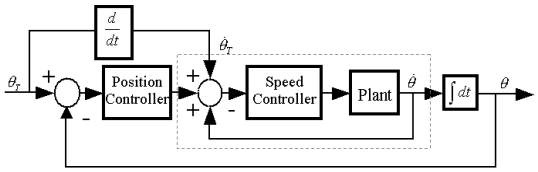

Fig. 2. Cascaded position control block diagram with embedded speed loop.

Embedding the speed controller in an outer position feedback loop gives a cascaded position controller designed to follow the reference trajectory $\theta_T(t)$. The cascaded structure around the speed loop compensates for any position error. It can be shown that a *PI* speed controller with a simple gain position controller has the low frequency characteristics of a *PID* controller.

Robots, in general, suffer from model uncertainty. For example, assuming the input is the current injected to each motor and the output is the angle of each link, the robot transfer function matrix for an extended arm configuration is not the same as that for a retracted arm configuration. Moreover, the robot's transfer function matrix depends on its load. Using a *PID* controller for the speed control of each motor, it may not be possible to achieve desirable gain and phase margins for a set of robot models simultaneously. An advanced controller offers the possibility of shaping the closed-loop system performance to achieve the desired margins as well as higher bandwidth and lower sensor noise in comparison to a *PID* controller.

1.2 Scope

The design of advanced controllers is discussed in Section 2. Sections 3 and 4 present results of laboratory tests comparing *PI* controllers and advanced controllers. Section 3 focuses on time-domain results, whereas Section 4 utilizes frequency-domain tools to compare the controllers. Section 5 presents results for the case of cascaded position control. Conclusions are drawn in Section 6.

2 ADVANCED CONTROLLER DESIGN

2.1 Introduction

The term "advanced controllers" is used to denote controllers with higher order structure than classical *PID*-type controllers. They do not offer the simplicity of only two tuning parameters for a *PI* controller or three parameters for a *PID* controller. With many "degrees-of-freedom" in terms of parameters to be adjusted, advanced controllers generally require an automated design suite for selection of parameters, i.e., tuning. Advanced controllers can be comprised of low-pass filters, notch filters, and lead and lag elements, singly or in combinations.

Motivation for Low-Pass Filters. Low-pass filters are generally employed to filter out sensor noise, at the possible expense of lowering the bandwidth. However, low-pass filters can be used to increase the bandwidth when high frequency resonances appear. This can be demonstrated by considering a *PI* controller used with a plant whose model includes high frequency resonances. The open-loop magnitudes at the resonant frequencies should be below 0 dB to ensure closed loop stability (essential when the plant's phase is highly uncertain, but still useful for a plant with low phase uncertainty). For a *PI* controller, e.g., a speed controller in Fig. 2 of the form $K_I/s + K_P$, stability will be limited by the fact that the plant amplitude around the resonant frequencies multiplied by K_P should be below 0 dB, although bounding K_P will limit the bandwidth. Adding a low-pass filter to the controller can effectively decrease the open-loop amplitude near the high frequency resonances and therefore increase the open-loop bandwidth. Another advantage of using a low-pass filter is to decrease noise effects at the plant input and output, at the expense of bandwidth.

Motivation for Notch Filters. Notch filters can be used to address problems of resonances. In general, resonances appearing at very low frequencies where the open-loop amplitude is much higher than 0 dB can be "notched" by closed-loop feedback and do not

require special treatment, e.g., use of a notch filter. Resonances appearing at high frequencies, that is, with open-loop amplitude below 0 dB and phase much below −180°, can be treated by notch filters to increase the bandwidth, as explained above for low-pass filters. Notch filters can also be used to increase the open-loop bandwidth for resonances appearing in an intermediate frequency range, where the open-loop phase is around −180°. A notch filter can decrease the open-loop amplitude, which should be below 0 dB in order to have reasonable phase margin, to increase the bandwidth.

Motivation for Lead and Lag Elements. Lead and lag elements are useful for satisfying system specifications. As indicated above, robots generally suffer from model uncertainty, and it may not be possible to simultaneously achieve desirable design specifications, such as gain and phase margins and bandwidth, for a set of robot models using a *PID* controller for each motor. Simultaneously satisfying design specifications can be accomplished with a controller with lead and/or lag elements. Here it is possible to shape the controller of uncertain plants in a way that the closed-loop system will have a desired margins, larger bandwidth, and lower sensor noise compared to a *PID* controller.

2.2 Identification

PID controllers and even *PID* controllers augmented with low-pass filters may not have sufficient degrees-of-freedom to satisfy all design specifications. They may suffer from performance limitations including having more gain and phase margin and robustness than required, and insufficient freedom to modify the design at low and high frequencies (e.g., high frequency roll-off). Advanced controllers can overcome these limitations by matching (or nearly matching) the desired robustness and margins (with no "over-design") and the desired roll-off and low frequency behavior. The first step in the design of an advanced controller is identification of the amplitude and phase of the plant's transfer function as a function of frequency (up to the Nyquist frequency for a digital design). Identification generally is straightforward at intermediate frequencies. Difficulties arise in the identification process at low frequencies (due to friction and plant maneuver limitations), at very high frequencies (due to sensor noise and quantization errors), and at and around resonant frequencies (due to model uncertainty).

For the experimental robot studied here an identification procedure was conducted covering approximately 300 frequencies (not equally spaced, denser around resonances) up to the Nyquist frequency. The robot has two motors and four sensors (two tachometers and two encoders), and thus can be described mathematically in terms of eight transfer functions where the input is the current to each motor and the output is the signal measured at each sensor. The results, summarized in Bode plots (not shown), indicate that motor 1 (i.e., the motor 1 and link 1 combination) has four dominant resonant frequencies ranging from 30 to 500 Hz, and motor 2 (i.e., the motor 2 and link 2 system) has a single dominant resonant frequency at about 16 Hz. These resonant frequencies limit the performance of *PI* controllers. Advanced controllers with notch and low-pass filters can attenuate the resonant frequencies, and actively damp some resonant modes.

Whereas the tachometers are mounted rigidly to the motor shafts, the encoders are mounted on flexible couplings (hidden from view in Fig. 1). Due to the compliant coupling, at some frequencies the interaction between the axes is so large that the effect of the current injected to motor 1 on its shaft is much lower than the effect on the shaft of motor 2. For currents introduced to motor 1, whose spectral densities are mainly around 200 Hz and 300 Hz, the tachometer located on motor 2 reads a signal up to 5 times larger than the tachometer located on motor 1. For currents injected to motor 2, whose spectral densities are around 200 Hz, the tachometer of motor 1 reads a signal of the same amplitude as that of motor 2.

2.3 Design of Controller

A speed controller that includes lead-lag elements, notch filters, and low-pass filters is proposed. With one of each of these, the speed controller transfer function for each motor will have the following continuous form structure

$$C(s)=\overbrace{\left(K_P+\frac{K_I}{s}\right)}^{PI}\ \overbrace{\frac{1+s/a}{1+s/b}}^{Lead}\ \times\ \overbrace{\frac{s^2+2\xi_1\omega_1 s+\omega_1^2}{s^2+2\xi_2\omega_1 s+\omega_2^2}}^{Notch}\ \overbrace{\frac{\omega_3^{\ 2}}{s^2+2\xi_3\ \ \omega_3 s+\omega_3^{\ 2}}}^{Low-pass}$$

and in discrete form (elements not normalized)

$$C(z)=\overbrace{\left(K_P+\frac{K_I z}{z-1}\right)}^{PI}\ \overbrace{\frac{z-a}{z-b}}^{Lead}\ \times\ \overbrace{\frac{z^2+\alpha_1 z+\beta_1}{z^2+\alpha_2 z+\beta_2}}^{Notch}\ \overbrace{\frac{z^2}{z^2+\alpha_3 z+\beta_3}}^{Low-pass}$$

(The controller transfer function matrix is assumed to be diagonal.) With this model, there are ten free parameters that must be tuned for the speed control of each motor. A special purpose software design suite was developed, based on the guidelines presented in this Section, that determines these parameters for the required performance such as gain and phase margins, bandwidth, and sensor noise. Using an algorithm relying on weighted optimization and AI rules, the software trades off the parameters to provide a controller design solution. It would be a

formidable task to complete the design manually, and there are no quick guidelines available, as is the case in *PID*-based designs.

3. SPEED CONTROL: TIME-DOMAIN

Tests of the robot with a *PI* speed controller proved quite challenging. Not only did the robot suffer from a strong limit cycle behavior (attributed to friction), it exhibited significant coupling between its axes. Using traditional *PI* tuning methods applied to one axis with the other axis inactive gave an integrated system that was not sufficiently robust. Even with successful tuning giving stable behavior, the robot suffered both gain and phase margin losses due to interaction of the axes. Traditional *PI* tuning methods applied to each axis with the other axis also active (tuned sequentially by *PI* methods), again gave a non-robust solution, while sacrificing both gain and phase margins.

To improve performance, the *PI* controller was augmented with a high frequency low-pass pole. With this modified *PI* controller it was possible to achieve robust robot motions with specified gain and phase margins. A *PI* plus low-pass controller was used to avoid the problems with friction and to increase the bandwidth. Results of tests with this *PI* plus low-pass controller and an advanced controller are discussed below.

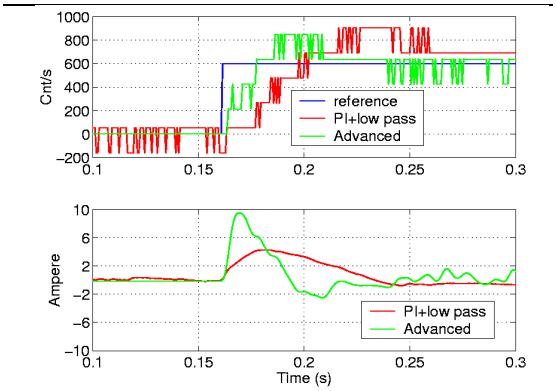

Fig. 3. Comparison between *PI* plus low-pass controller and advanced controller. Step command to motor 1 is 600 counts/s, and to motor 2 zero.

The robot was tested for several speed reference commands. Fig. 3 shows the step response of motor 1 with the *PI* plus low-pass controller and the advanced controller. The tracking error, rise time and settling time of the advanced controller are much lower than the corresponding results of the *PI* plus low-pass controller. The rise time of the advanced controller is 0.017s, or 43% of the 0.040s rise time of the *PI* plus low-pass controller. The improvement in performance of the advanced controller occurs with the penalty of increased current (twice the peak current) and larger high frequency noise. In Fig. 3 the measured speed was obtained by differentiating the encoder signal.

The results for motor 2 (not shown) also demonstrate that the tracking error, rise time, and settling time of the advanced controller are much lower than that of the *PI* plus low-pass controller. The rise time of the advanced controller is 0.02s, or one-fifth of the 0.1s rise time of the *PI* plus low-pass controller. The price for the higher performance of the advanced controller is again an increase in the peak current and overshoot. In general, the peak current depends on the command trajectory, which is usually smooth (not a step). For example, Fig. 4 compares the performance of the advanced controller and the *PI* plus low-pass controller for an acceleration limited (i.e., ramp) speed command, and shows the peak current is about the same for both controllers. Again, the tracking error for the advanced controller is much lower than for the *PI* plus low-pass controller.

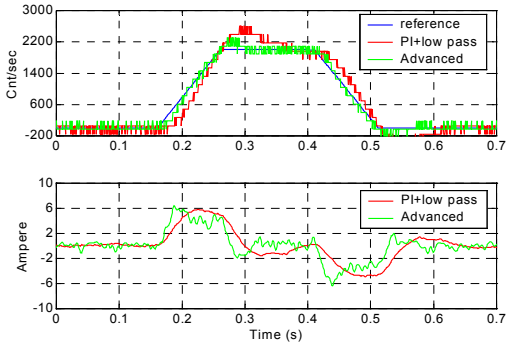

Fig. 4. Comparison between *PI* plus low-pass controller and advanced controller. Trajectory command to motor 1 is 2000 counts/s, acceleration limitation 20000 counts/s^2. Motor 2 is commanded to stop.

4. SPEED CONTROL: FREQUENCY DOMAIN

In section 3 the robot's tracking performance for different controllers was studied. The controller was subjected to step and ramp reference waveforms to determine the transient behavior of the closed-loop system. These time-domain tests demonstrate the improvement in performance of the real (non-linear) system using an advanced controller that was designed based on a linear model. A frequency analysis of the linear system, using Bode and Nichols plots, was conducted to address questions such as the feasibility of better designs and the amount of robustness and margins available.

Some properties of a closed-loop feedback system can be estimated from the open-loop transfer function, such as the rise time, settling time, and robustness to plant changes. In addition, comparisons

between different controllers can be made in terms of amplification of the sensor noise at the plant input.

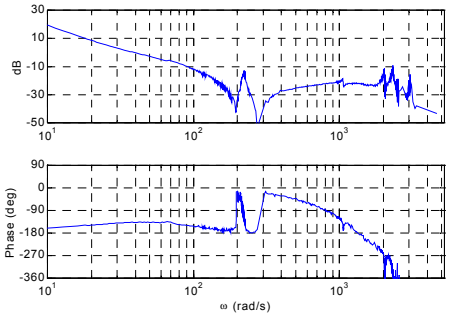

Fig. 5. Open-loop Bode plot of motor 1 using *PI* and low-pass controller

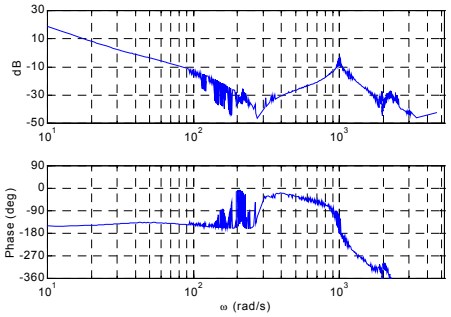

Fig. 6. Open-loop Bode plot of motor 2 using *PI* and low-pass controller

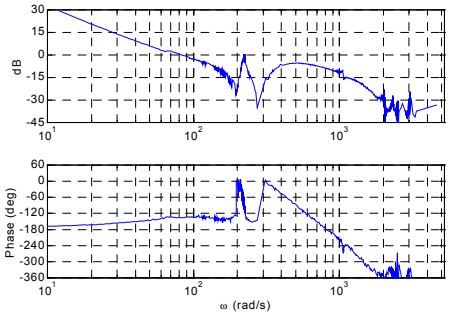

Fig. 7. Open-loop Bode plot of motor 1 using advanced controller

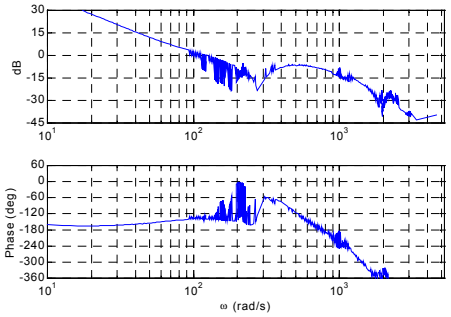

Fig. 8. Open-loop Bode plot of motor 2 using advanced controller

In the interest of enhanced understanding of the closed-loop system, open-loop Bode plots for motors 1 and 2 for the *PI* plus low-pass controllers were generated, as shown in Figs. 5 and 6, respectively. Correspondingly, open-loop Bode plots for motors 1 and 2 for the advanced controllers are shown in Figs. 7 and 8, respectively. Several conclusions can be drawn from these figures:

1. The bandwidth of the advanced controller for motor 1 is about 15 Hz, almost 2.5 larger than the 6.2 Hz of the *PI* controller.
2. The bandwidth of the advanced controller for motor 2 is about 13 Hz, almost 2.5 larger than the 5.7 Hz of the *PI* controller.
3. The low frequency disturbance attenuation of the advanced controller for motor 1 is 5 times better than that of the *PI* controller.
4. The low frequency disturbance attenuation of the advanced controller for motor 2 is 10 times better than that of the *PI* controller.

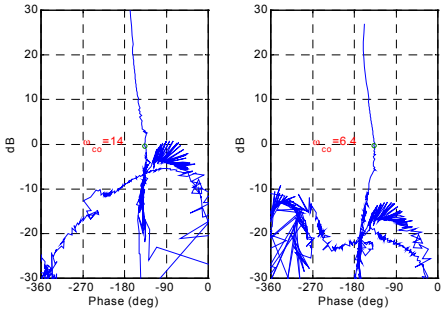

Fig. 9. Open-loop Nichols plots of speed controller of motor 1, left advanced, right *PI* plus low-pass. Crossover frequencies are 14 Hz and 6.2 Hz, respectively.

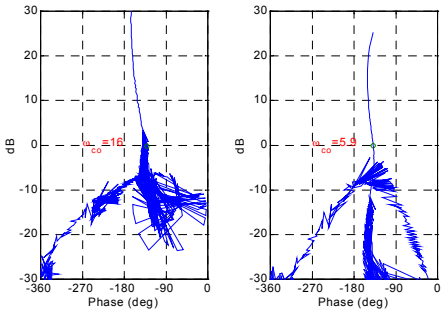

Fig. 10. Open-loop Nichols plots of speed controller of motor 2, left advanced, right *PI* plus low-pass. Gain and phase margins are about the same, crossover frequencies are 16 Hz and 5.2 Hz, respectively.

The Nichols charts of Figs. 9 and 10 are presented to demonstrate that a fair comparison was made, in the sense that similar gain and phase margins were taken

for the *PI* plus low-pass and the advanced controllers. Fig. 10 compares the open-loop response for motor 2 for the advanced controller and the *PI* plus low-pass controller. Both have the same gain and phase margins of approximately 8 dB and 35 deg, respectively. Fig. 9 shows a similar comparison for motor 1 with the margins again being the same. It is impossible to increase the gain of the *PI* controller and maintain the same margins since: (i) the phase margin will be less than the required 35 deg, and (ii) the resonance whose gain is about 9 dB is highly phase uncertain.

5. POSITION CONTROL

In addition to the speed control comparisons addressed in Sections 3 and 4, tests were conducted to investigate cascaded position control. In the controllers explored here, the speed controller was either the *PI* plus low-pass controller or the advanced controller of sections 2 and 3, and the position controller was a simple gain. Fig. 11 presents test results for a step command limited by speed and acceleration for motor 1. The comparison shows that for both motors the advanced controller tracks the reference command better than the cascaded *PI* plus low-pass controller. In addition, the current consumed by both controllers is approximately the same with the same peak value.

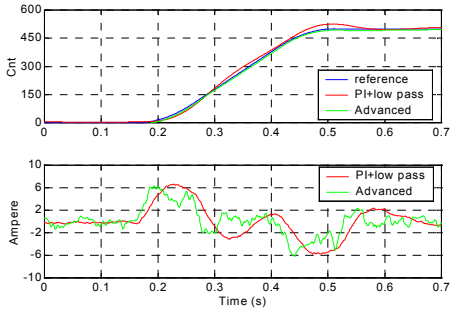

Fig. 11. Comparison between *PI* plus low-pass controller and advanced controller. The trajectory command for motor 1 is 500 counts with speed and acceleration limitation of 2000 counts/s and 20000 counts/s^2, respectively. Motor 2 commanded to stop.

A movie demonstrating the performance of the robot under cascaded position control with the advanced speed controller can be seen at the web site: `www.eng.tau.ac.il/~yaniv`.

6. CONCLUSIONS

A robotic application was used to compare the performance of an advanced controller relative to a classical controller. The classical controller even augmented with a notch filter could not meet the performance achievable by the advanced controller in terms of bandwidth, settling time and low-frequency disturbance rejection. For the robotic system tested the results demonstrate clear advantages in adopting the advanced controller.

In practice, controller designs of higher order than the classical *PID*-type can often be useful. To effectively design an advanced controller, an accurate identification must first be conducted, and an automated controller design system must be available. In this work, an identification and design environment were developed that can (i) identify the dynamics of a complex mechanical system, including inter-axis coupling and uncertainty, and (ii) design the controller (e.g., select the structure and tune the controller parameters) based on the identification using "loop shaping" AI-based controller design software. The resulting design is used for programming the motor controllers.

In many real-world applications, classical control (*PI* or *PID* designs) may not be sufficient to achieve the desired performance. Significant improvements in performance can be afforded by using advanced controllers with many free design parameters. However, for advanced controllers, there are no quick guidelines for setting parameters and tuning must be based on software that relies on identification of the physical system dynamics. This identification should be carefully executed, and include system uncertainties such as amplifier limitations, robot geometry, uncertainty around resonances, etc.

ACKNOWLEDGEMENTS

Prof. Nagurka (Marquette University) is grateful for a Fulbright Scholarship for the 2001-2002 academic year allowing him to pursue this research with Prof. Flash (The Weizmann Institute) and Prof. Yaniv (Tel-Aviv University).

REFERENCES

Faye, I.C. (1986). An Impedance Controlled Manipulandum for Human Movement Studies. *M.S. Thesis*, MIT, Cambridge, MA.

Flash, T. (1987). The Control of Hand Equilibrium Trajectories in Multi-Joint Arm Movements. *Biological Cybernetics*, Vol. 57, pp. 257-274.

Mann, G.K.I., Hu, B.G., and Gosine, R.G. (2001). Time-domain based design and analysis of new PID tuning rules. *IEE Proc. Control Theory Appl.,* Vol. 148, No. 3, pp.251-261.

Mussa-Ivaldi, F.A., Hogan, N., and Bizzi, E. (1985). Neural, Mechanical, and Geometric Factors Subserving Arm Posture in Humans. *J. Neuroscience*, Vol. 5, No. 1 , pp. 2732-2743.

Won, J. and Hogan, N. (1995). Stability Properties of Human Reaching Movements. *Experimental Brain Research*, Vol.107, No. 1, pp. 125-136.